

Electron Spin Resonance and Electron Spin Echo Modulation Spectroscopic Studies of Cupric Ion–Adsorbate Interactions in Synthetic Clinoptilolite

Dongyuan Zhao,[†] Rosemarie Szostak,[‡] and Larry Kevan^{*,†}

Department of Chemistry, University of Houston, Houston, Texas 77204-5641, and Department of Chemistry, Clark Atlanta University, Atlanta, Georgia 30314

Received: February 25, 1997; In Final Form: April 14, 1997[⊗]

The site locations and adsorbate interactions of Cu²⁺ in Cu²⁺-exchanged synthetic clinoptilolite have been determined by electron spin resonance and electron spin echo modulation spectroscopies. Strong effects of the H⁺, Li⁺, Na⁺, and K⁺ cocations have been found on the coordination number and on the location of the cupric ion. Cu²⁺ coordinates three molecules of water in hydrated CuH–clinoptilolite (CuH–Clino) and in CuLi–Clino, but only two molecules of water in hydrated CuNa–Clino and CuK–Clino. Two cupric ion sites are observed in many cases and are attributed to sites in ten-ring and eight-ring main channels. Activation to 400 °C is sufficient to remove these water molecules and cause migration of Cu²⁺ to an eight-ring intersecting channel. Adsorption of polar molecules such as water, ammonia, alcohols, and acetonitrile causes the migration of Cu²⁺ into the main channels to coordinate with the adsorbates. Cu²⁺ forms complexes with three molecules of ethanol and four of ammonia in CuH–Clino, but only coordinates to two molecules of ethanol or methanol and three of ammonia in CuNa–Clino, and to one molecule of ethanol or methanol and three of ammonia in CuK–Clino. Cu²⁺ coordinates four molecules of acetonitrile at the center of a main channel in clinoptilolite, and this coordination number is unaffected by the alkali metal cocations.

Introduction

Zeolites exchanged with cupric ion have stimulated interest in their use as catalysts for oxidation^{1–5} and NO reduction.⁶ The nature of that catalytic activity depends both on the location of the cupric ion and on its interaction with adsorbates.⁷ In the case of paramagnetic Cu²⁺ species, much information concerning both of these aspects may be gleaned from electron spin resonance (ESR) and electron spin echo modulation (ESEM) spectroscopy.^{8–13} ESR gives information about the symmetry of a complex while ESEM gives quantitative information about adsorbate coordination numbers and geometry.

Clinoptilolite is the most abundant natural zeolite and has found applications in ion exchange, adsorption, and catalysis.^{14–17} However, paramagnetic iron impurities commonly found in natural clinoptilolite limit characterization of other paramagnetic transition metal ions by ESR and ESEM spectroscopies. We have succeeded in synthesizing clinoptilolite without seed crystals which does not contain detectable Fe³⁺ impurity¹⁸ to enable us to report the first studies on cupric ion location and adsorbate interactions in clinoptilolite.

Effects of the cocation (H⁺, Na⁺, K⁺, or Ca²⁺) upon Cu²⁺ ion sites in ZSM-5 zeolite and in mordenite have been shown by ESR and ESEM.^{19–21} ZSM-5 is a pentasil zeolite that consists of a three-dimensional channel system, while mordenite consists of a 12-member ring main channel that is intersected by a series of smaller channels.¹⁹ Cupric ion was found to form large complexes with methanol and ethanol in H–ZSM-5 and H–mordenite but could not coordinate to as many alcohol molecules when the cocation was Na⁺, K⁺, or Ca²⁺. It was concluded that the complexes formed between Cu²⁺ and alcohol adsorbates could only be accommodated at channel intersections where there is adequate free space for such complexes.²¹

In contrast to ZSM-5 and mordenite, clinoptilolite consists of A (10-member ring) and B (eight-member ring) main

channels parallel to each other and to the *c*-axis of the unit cell, while C channels (eight-member ring) intersect the A and B channels.^{14,22} It is of interest to examine the location of Cu²⁺ and the effect of the cocation in synthetic clinoptilolite by studying the complexes formed between Cu²⁺ and various adsorbates.

In this study, the interactions between Cu²⁺ and water, methanol, ethanol, ammonia, pyridine, acetonitrile and ethylene adsorbates in H–clinoptilolite (H–Clino), Li–clinoptilolite (Li–Clino), Na–clinoptilolite (Na–Clino), and K–clinoptilolite (K–Clino) are characterized. ESR and ESEM results reveal substantial cocation effects on the coordination of various adsorbates.

Experimental Section

Synthesis. Clinoptilolite zeolites were prepared as follows¹⁸ in stainless steel autoclaves lined with Teflon under autogenous pressure from the gel. In a typical synthesis, 0.78 g of dried aluminum hydroxide, Al(OH)₃ (USP, Pfaltz & Bauer Inc.), was added to 0.59 g of 6 N NaOH and 2.80 g of 6 N KOH solution with stirring. After stirring for 0.5 h, 10 g of colloidal silica solution (Ludox LS 30 wt %, silica, Aldrich Chemical Corp.) was added with strong stirring for 1 h. This gel was placed in a static autoclave at 180 °C for 112 h; the final pH of the product was 11.7. After cooling to room temperature the resulting solid product was recovered by filtration on a Buchner funnel, washed with water, and dried in air at 70 °C. The sample was characterized by X-ray powder diffraction (Siemens D5000 diffractometer) and electron microprobe analysis (JEOL JXA 8600 Superprobe). The unit cell contents were determined to be Na_{0.62}K_{5.37}[Al_{6.0}Si_{30.0}O₇₂].

Ion Exchange. The synthetic Na,K–clinoptilolite was exchanged with 1.0 M ammonium chloride at 70 °C overnight, followed by washing. This procedure was repeated two times. The product was calcined in air at 400 °C overnight to obtain H–Clino. Na–Clino, Li–Clino, or K–Clino were prepared

[†] University of Houston.

[‡] Clark Atlanta University.

[⊗] Abstract published in *Advance ACS Abstracts*, June 15, 1997.

TABLE 1: ESR Parameters for Cupric Ion at 77 K in Synthetic Clinoptilolite for Various Sample Pretreatment Conditions^a

sample pretreatment	cation			
	H ⁺	Li ⁺	Na ⁺	K ⁺
fresh ^b	$g_{\parallel} = 2.400, A_{\parallel} = 137$ $g_{\perp} = 2.366, A_{\perp} = 148$ $g_{\perp} = 163, g_{\perp} = 2.045$	$g_{\parallel} = 2.390, A_{\parallel} = 136$ $g_{\perp} = 2.165$ $g_{\perp} = 2.065$	$g_{\parallel} = 2.402, A_{\parallel} = 128$ $g_{\perp} = 2.163$ $g_{\perp} = 2.067$	$g_{\parallel} = 2.375, A_{\parallel} = 151$ $g_{\perp} = 2.164$ $g_{\perp} = 2.067$
fresh	$g_{\parallel} = 2.373, A_{\parallel} = 168$ $g_{\parallel} = 2.417, A_{\parallel} = 147$ $g_{\perp} = 2.061$	$g_{\parallel} = 2.428, A_{\parallel} = 128$ $g_{\parallel} = 2.401, A_{\parallel} = 136$ $g_{\perp} = 2.061$	$g_{\parallel} = 2.430, A_{\parallel} = 126$ $g_{\parallel} = 2.391, A_{\parallel} = 145$ $g_{\perp} = 2.061$	$g_{\parallel} = 2.406, A_{\parallel} = 137$ $g_{\parallel} = 2.389, A_{\parallel} = 145$ $g_{\perp} = 2.059$
calc, 300 °C	$g_{\parallel} = 2.373, A_{\parallel} = 167$ $g_{\parallel} = 2.418, A_{\parallel} = 149$ $g_{\perp} = 2.060$	$g_{\parallel} = 2.429, A_{\parallel} = 127$ $g_{\parallel} = 2.397, A_{\parallel} = 135$ $g_{\perp} = 2.057$	$g_{\parallel} = 2.430, A_{\parallel} = 125$ $g_{\parallel} = 2.388, A_{\parallel} = 145$ $g_{\perp} = 2.058$	$g_{\parallel} = 2.389, A_{\parallel} = 147$ $g_{\parallel} = 2.406, A_{\parallel} = 137$ $g_{\perp} = 2.055$
in air	$g_{\parallel} = 2.401, A_{\parallel} = 146$ $g_{\perp} = 2.061$	$g_{\parallel} = 2.376, A_{\parallel} = 150$ $g_{\perp} = 2.057$	$g_{\parallel} = 2.401, A_{\parallel} = 143$ $g_{\perp} = 2.055$	$g_{\parallel} = 2.389, A_{\parallel} = 145$ $g_{\perp} = 2.055$
calc, 450 °C	$g_{\parallel} = 2.392, A_{\parallel} = 147$ $g_{\perp} = 2.056$	$g_{\parallel} = 2.364, A_{\parallel} = 148$ $g_{\perp} = 2.050$	$g_{\parallel} = 2.366, A_{\parallel} = 149$ $g_{\perp} = 2.046$	$g_{\parallel} = 2.389, A_{\parallel} = 137$ $g_{\perp} = 2.045$
in air	$g_{\parallel} = 2.393, A_{\parallel} = 146$ $g_{\parallel} = 2.314, A_{\parallel} = 186$ $g_{\perp} = 2.056$	$g_{\parallel} = 2.396, A_{\parallel} = 153$ $g_{\parallel} = 2.313, A_{\parallel} = 195$ $g_{\perp} = 2.061$	$g_{\parallel} = 2.396, A_{\parallel} = 146$ $g_{\parallel} = 2.314, A_{\parallel} = 163$ $g_{\perp} = 2.059$	$g_{\parallel} = 2.371, A_{\parallel} = 153$ $g_{\parallel} = 2.316, A_{\parallel} = 177$ $g_{\perp} = 2.058$
evac RT	$g_{\parallel} = 2.310, A_{\parallel} = 184$ $g_{\parallel} = 2.308, A_{\parallel} = 164$	$g_{\parallel} = 2.316, A_{\parallel} = 185$ $g_{\parallel} = 2.290, A_{\parallel} = 165$	$g_{\parallel} = 2.317, A_{\parallel} = 169$	$g_{\parallel} = 2.316, A_{\parallel} = 176$
evac, 100 °C				
evac, 150 °C	$g_{\parallel} = 2.293, A_{\parallel} = 164$ $g_{\parallel} = 2.315, A_{\parallel} = 180$	$g_{\parallel} = 2.316, A_{\parallel} = 182$ $g_{\parallel} = 2.290, A_{\parallel} = 164$	$g_{\parallel} = 2.320, A_{\parallel} = 165$ $g_{\parallel} = 2.315, A_{\parallel} = 165$	$g_{\parallel} = 2.310, A_{\parallel} = 176$ $g_{\parallel} = 2.313, A_{\parallel} = 178$
evac, 250 °C	$g_{\parallel} = 2.287, A_{\parallel} = 164$ $g_{\parallel} = 2.286, A_{\parallel} = 163$ $g_{\parallel} = 2.315, A_{\parallel} = 182$	$g_{\parallel} = 2.314, A_{\parallel} = 188$ $g_{\parallel} = 2.291, A_{\parallel} = 165$	$g_{\parallel} = 2.320, A_{\parallel} = 169$ $g_{\parallel} = 2.263, A_{\parallel} = 148$	$g_{\parallel} = 2.314, A_{\parallel} = 178$ $g_{\parallel} = 2.263, A_{\parallel} = 148$
evac, 400 °C				
400 °C, O ₂				

^a RT = room temperature, calc = calcined, evac = evacuated, units of A_{\parallel} are $\times 10^{-4} \text{ cm}^{-1}$. ^b ESR at room temperature instead of 77 K.

by exchanging three times with 1 M solutions of NaCl, LiCl, or KCl at 70 °C overnight.

All samples were doped with Cu²⁺ by adding 10 mL of 10^{−3} M Cu(NO₃)₂ to 1 g of clinoptilolite and 100 mL of deionized water. The samples were filtered and washed thoroughly with hot deionized water and then allowed to air-dry. Samples prepared in this manner are referred to as “fresh”. The clinoptilolite structure was retained after ion exchange and calcination according to X-ray powder diffraction.

ESR and ESEM Measurements. Samples were activated in 2 mm i.d. \times 3 mm o.d. Suprasil quartz tubes that were attached to a vacuum line. Activation or dehydration of clinoptilolite was carried out by first evacuating the zeolite at room temperature. The temperature was then raised slowly over an 8 h period to 400 °C. The samples were exposed to 600 Torr of ultrahigh-purity oxygen to reoxidize any Cu²⁺ that was reduced during the activation process. After 2 h the oxygen was pumped off to a pressure of 1×10^{-5} Torr, and the samples were cooled to room temperature.

D₂O, CD₃CN, and C₂H₅OD (Aldrich), CD₃OH and ND₃ (Stohler), and CD₂CD₂ and C₅D₅N (Linde) were used as adsorbates after purification by several freeze–pump–thaw cycles. The samples after activation were equilibrated with the saturated room-temperature vapor pressure of the liquids, while 400 Torr of gaseous C₂H₄ and ND₃ was used. After equilibration, the samples were frozen in liquid nitrogen and sealed.

Continuous-wave ESR spectra were recorded on a Bruker 380 pulsed ESR spectrometer at both room temperature and 77 K. Several scans (5–10) per sample were averaged. ESEM spectra were recorded at 5 K on the same spectrometer using an Oxford Instruments CF 935 flowing liquid helium cryostat. Three-pulse stimulated spin echoes were recorded with a $\pi/2$, $\pi/2$, $\pi/2$ pulse sequence in which the echo intensity was measured as a function of the time, T , between the second and third pulses. The value for τ , the time between the first and second pulses, was selected to minimize modulation from ²⁷Al nuclei contained in the clinoptilolite lattice. Phase cycling was employed to correct for the two pulse glitches that occur at $T = \tau$ and $T = 2\tau$.¹³

The ESEM spectra were simulated with a ratio analysis procedure that has been described in detail elsewhere.^{12,23} The value for N , the number of nearest equivalent nuclei around the paramagnetic center, was constrained to be integral. In general, N can then be determined uniquely up to about $N = 10$, while the value for R , the distance from the paramagnetic center to the nuclei, is determined to ± 0.01 nm.

Results

Effect of Calcination. The synthetic clinoptilolite zeolites after ion exchange with NH₄⁺, Li⁺, Na⁺, or K⁺ and copper(II) doping after calcination at 600 °C have similar X-ray diffraction patterns to natural clinoptilolite zeolite.¹⁸ This agrees with the discussion of Mumpton²⁴ and verifies that clinoptilolite is thermally stable.

A complete list of ESR parameters at 77 K for the variously exchanged clinoptilolites is given in Table 1. The hyperfine splitting is only recorded in the g_{\parallel} region of the spectrum since it is generally unresolved in the g_{\perp} region. Figure 1 shows the change of ESR spectra upon calcination of CuH–Clino and CuNa–Clino at 300, 450, and 600 °C in air. In a fresh CuH–Clino sample, two main species are observed at 77 K with ESR parameters $g_{\parallel} = 2.373, A_{\parallel} = 168 \times 10^{-4} \text{ cm}^{-1}$ and $g_{\parallel} = 2.417, A_{\parallel} = 147 \times 10^{-4} \text{ cm}^{-1}$. At room temperature the ESR spectrum is broader with less resolved copper hyperfine splitting, and another isotropic species at $g = 2.164$ seems to be observed. After calcination in air and rehydration, the intensity of the ESR spectrum decreases, and the species at $g_{\parallel} = 2.373$ almost disappears.

In fresh CuLi–Clino, CuNa–Clino, and CuK–Clino, two similar main Cu²⁺ species are observed at 77 K with slightly higher g_{\parallel} and smaller A_{\parallel} as shown in Table 1. At room temperature the ESR spectrum of CuNa–Clino (Figure 1B) is similar, but only one Cu²⁺ species is resolved in the g_{\parallel} region; in addition, a broad isotropic signal at $g_{\text{iso}} = 2.163$ and 2.164 is observed for fresh CuNa–Clino and CuK–Clino, respectively. After calcination at 300 °C in air and rehydration, two Cu²⁺ species at $g_{\parallel} = 2.388, A_{\parallel} = 145 \times 10^{-4} \text{ cm}^{-1}$ and $g_{\parallel} =$

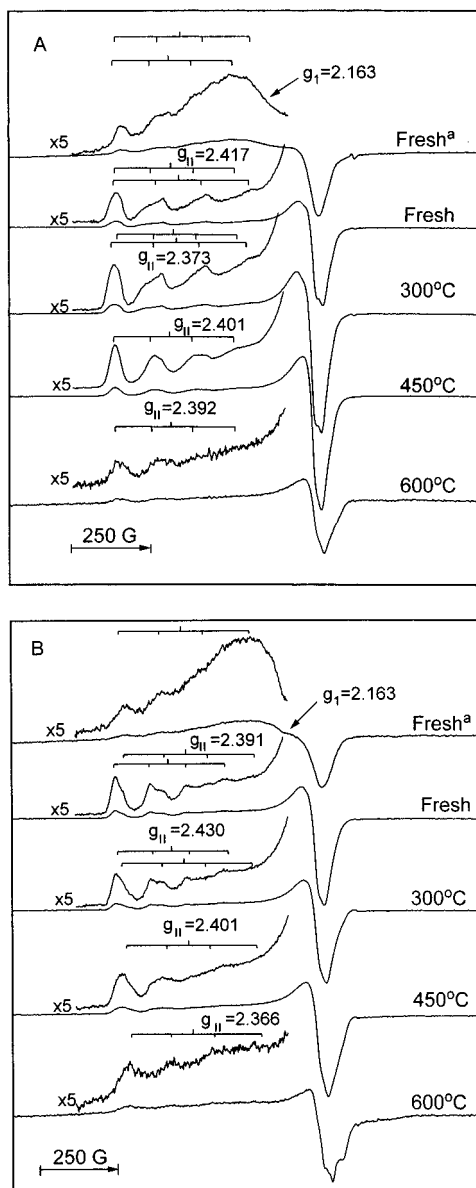


Figure 1. ESR spectra at 77 K except for the fresh^a sample at room temperature of (A) CuH-clinoptilolite and (B) CuNa-clinoptilolite with calcination at 300, 450, and 600 °C in air.

2.430, $A_{||} = 125 \times 10^{-4} \text{ cm}^{-1}$ are observed in CuNa-Clino (Figure 1B). After calcination at 450 and 600 °C, only one Cu^{2+} species is resolved. CuLi-Clino and CuK-Clino show similar results to CuNa-Clino, as shown in Table 1.

When CuH-Clino is evacuated at room temperature, the species at $g_{||} = 2.417$ almost disappears, and the second species shows a slight shift in $g_{||}$ from 2.417 to 2.393 (Figure 2A). A new third species is also observed at $g_{||} = 2.314$, $A_{||} = 186 \times 10^{-4} \text{ cm}^{-1}$. At the same time, the ESR spectrum in the g_{\perp} region becomes somewhat resolved. Further dehydration at 100 °C causes the new third species to become dominant. Continued dehydration to 250 °C produces a fourth species with ESR parameters of $g_{||} = 2.293$, $A_{||} = 164 \times 10^{-4} \text{ cm}^{-1}$, which then becomes the dominant species. After complete dehydration by heating to 400 °C only this fourth species remains. Exposure to oxygen at 400 °C recovers the third species which becomes dominant. The changes in the ESR spectra for CuLi-Clino with dehydration are similar to those of CuH-Clino, except that after evacuation at 400 °C the Cu^{2+} signal is lost.

Evacuation of CuNa-Clino at room temperature shows similar changes in its ESR spectra (Figure 2B) at 77 K as those

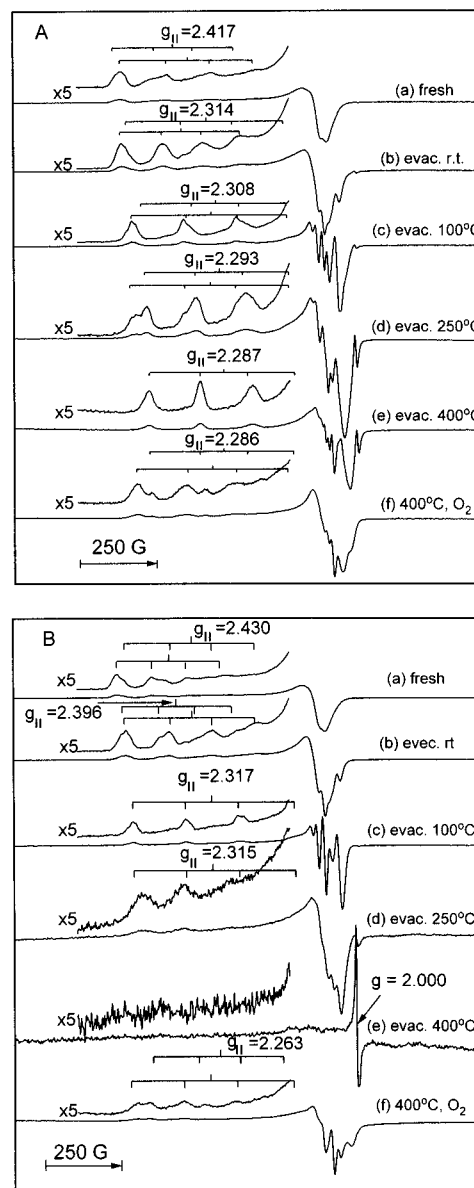


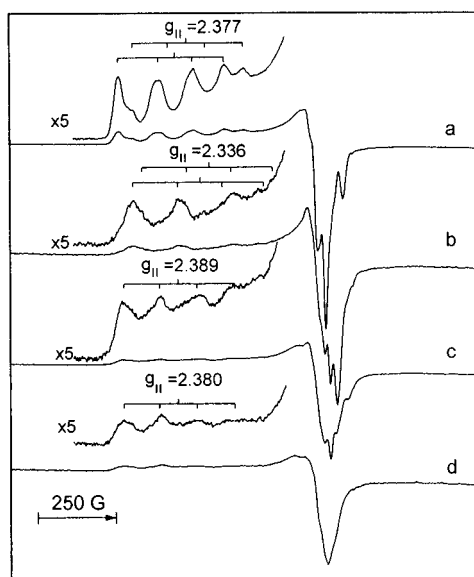
Figure 2. ESR spectra at 77 K of (A) CuH-clinoptilolite and (B) CuNa-clinoptilolite: (a) hydrated sample, (b) after subsequent evacuation at room temperature, (c) after subsequent evacuation at 100 °C, (d) after subsequent evacuation at 250 °C, (e) after subsequent evacuation at 400 °C, and (f) after subsequent evacuation at 400 °C for 8 h and exposure to 600 Torr of oxygen at 400 °C for 3 h.

of CuH-Clino. The Cu^{2+} species with $g_{||} = 2.396$, $A_{||} = 146 \times 10^{-4} \text{ cm}^{-1}$ becomes the dominant species. Further dehydration at 50 °C produces a third Cu^{2+} species with $g_{||} = 2.317$, $A_{||} = 169 \times 10^{-4} \text{ cm}^{-1}$. Continued dehydration at 100 °C causes the third Cu^{2+} species to become dominant, and after dehydration at 250 °C only this third Cu^{2+} species remains. After complete dehydration by heating to 400 °C, the Cu^{2+} signal is lost, and only a narrow signal at $g = 2.000$ remains which may be from a lattice defect. After heating at 400 °C in 600 Torr of O_2 for 3 h, the third Cu^{2+} species is recovered, and a new Cu^{2+} species with $g_{||} = 2.263$, $A_{||} = 148 \times 10^{-4} \text{ cm}^{-1}$ is observed. The ESR spectra of CuK-Clino after dehydration change similarly to those of CuNa-Clino (see Table 1), except that the second Cu^{2+} species remains after dehydration at 100 °C.

Adsorbate Interactions. Table 2 lists the ESR parameters of all cupric ion species formed by interaction with various adsorbates. Complete rehydration of activated clinoptilolite at room temperature regenerates the first and second Cu^{2+} species

TABLE 2: ESR Parameters for Cupric Ion at 77 K in Synthetic Clinoptilolite for Various Adsorbates^a

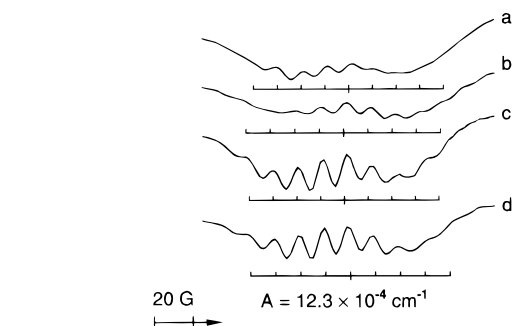
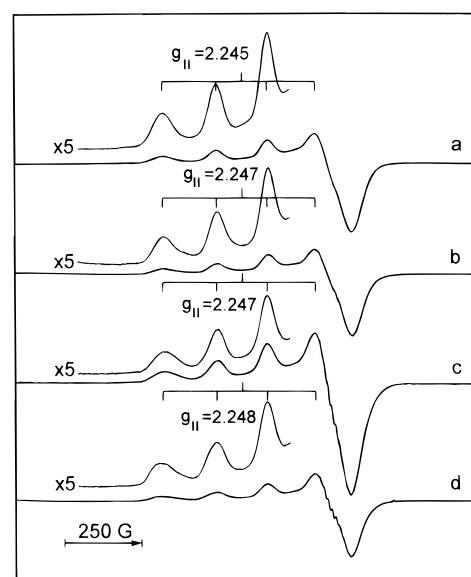
adsorbate	cocation			
	H ⁺	Li ⁺	Na ⁺	K ⁺
D ₂ O	$g_{ } = 2.379, A_{ } = 155$ $g_{ } = 2.410, A_{ } = 141$ $g_{\perp} = 2.059$	$g_{ } = 2.377, A_{ } = 155$ $g_{ } = 2.366, A_{ } = 140$ $g_{\perp} = 2.058$	$g_{ } = 2.386, A_{ } = 150$ $g_{ } = 2.427, A_{ } = 131$ $g_{\perp} = 2.059$	$g_{ } = 2.404, A_{ } = 146$ $g_{ } = 2.414, A_{ } = 138$ $g_{\perp} = 2.061$
C ₂ H ₅ OD	$g_{ } = 2.417, A_{ } = 136$ $g_{ } = 2.377, A_{ } = 134$ $g_{\perp} = 2.049$	$g_{ } = 2.336, A_{ } = 158$ $g_{ } = 2.372, A_{ } = 127$ $g_{\perp} = 2.049$	$g_{ } = 2.389, A_{ } = 145$	$g_{ } = 2.380, A_{ } = 144$
CD ₃ OD			$g_{\perp} = 2.042$ $g_{ } = 2.387, A_{ } = 140$ $g_{\perp} = 2.055$	$g_{\perp} = 2.043$ $g_{ } = 2.380, A_{ } = 144$ $g_{\perp} = 2.053$
ND ₃	$g_{ } = 2.245, A_{ } = 177$ $g_{\perp} = 2.044$	$g_{ } = 2.247, A_{ } = 177$ $g_{\perp} = 2.041$	$g_{ } = 2.247, A_{ } = 177$ $g_{\perp} = 2.046$	$g_{ } = 2.248, A_{ } = 177$ $g_{\perp} = 2.046$
C ₅ D ₅ N	$g_{ } = 2.329, A_{ } = 165$ $g_{ } = 2.269, A_{ } = 184$	$g_{ } = 2.309, A_{ } = 169$ $g_{ } = 2.317, A_{ } = 180$	$g_{ } = 2.323, A_{ } = 163$ $g_{ } = 2.262, A_{ } = 202$	$g_{ } = 2.314, A_{ } = 173$ $g_{ } = 2.277, A_{ } = 161$
CD ₃ CN	$g_{ } = 2.363, A_{ } = 146$	$g_{ } = 2.364, A_{ } = 147$ $g_{ } = 2.304, A_{ } = 174$ $g_{\perp} = 2.048$	$g_{ } = 2.361, A_{ } = 145$ $g_{ } = 2.320, A_{ } = 172$ $g_{\perp} = 2.043$	$g_{ } = 2.365, A_{ } = 146$
CD ₂ CD ₂	$g_{\perp} = 2.046$ $g_{ } = 2.358, A_{ } = 146$ $g_{ } = 2.295, A_{ } = 165$ $g_{\perp} = 2.049$	$g_{ } = 2.346, A_{ } = 148$ $g_{ } = 2.300, A_{ } = 161$ $g_{\perp} = 2.046$	$g_{ } = 2.322, A_{ } = 163$ $g_{ } = 2.353, A_{ } = 121$ $g_{\perp} = 2.053$	$g_{\perp} = 2.043$ $g_{ } = 2.314, A_{ } = 175$ $g_{ } = 2.255, A_{ } = 175$ $g_{\perp} = 2.060$

^a Units of $A_{||}$ are $\times 10^{-4} \text{ cm}^{-1}$.**Figure 3.** ESR spectra at 77 K after adsorption of ethanol (C₂H₅OD) on (a) CuH-clinoptilolite, (b) CuLi-clinoptilolite, (c) CuNa-clinoptilolite, and (d) CuK-clinoptilolite.

found in a fresh sample. The second Cu²⁺ species with $g_{||} = 2.377$ – 2.404 , $A_{||} = (146$ – $155) \times 10^{-4} \text{ cm}^{-1}$ becomes dominant.

The adsorption of ethanol onto CuH–Clino produces two main Cu²⁺ species at $g_{||} = 2.417$, $A_{||} = 136 \times 10^{-4} \text{ cm}^{-1}$ and $g_{||} = 2.377$, $A_{||} = 134 \times 10^{-4} \text{ cm}^{-1}$ as shown in Figure 3. The first species with $g_{||} = 2.417$ is dominant. None of the cupric ions remain uncomplexed, but the adsorption of ethanol to change the ESR spectra proceeds slowly relative to water. Two Cu²⁺ species are also observed in CuLi–Clino with $g_{||} = 2.336$, $A_{||} = 158 \times 10^{-4} \text{ cm}^{-1}$ and $g_{||} = 2.372$, $A_{||} = 127 \times 10^{-4} \text{ cm}^{-1}$ with the first species dominant. However, ethanol adsorbed onto CuNa–Clino and CuK–Clino produces only one Cu²⁺ species at $g_{||} = 2.380$ – 2.389 , $A_{||} = (144$ – $145) \times 10^{-4} \text{ cm}^{-1}$. When methanol is adsorbed onto CuNa–Clino and CuK–Clino, the same species are detected as for ethanol adsorption.

The adsorption of ND₃ onto CuH–Clino, CuLi–Clino, CuNa–Clino, and CuK–Clino produces a new Cu²⁺ species with $g_{||} = 2.245$ – 2.248 , $A_{||} = 177 \times 10^{-4} \text{ cm}^{-1}$, and $g_{\perp} = 2.041$ – 2.046 . Figure 4 shows the ESR spectra obtained from CuH–Clino, CuLi–Clino, CuNa–Clino, and CuK–Clino samples after ND₃ adsorption. Nine nitrogen hyperfine lines

**Figure 4.** ESR spectra at 77 K after adsorption of ammonia (ND₃) on (a) CuH-clinoptilolite, (b) CuLi-clinoptilolite, (c) CuNa-clinoptilolite, and (d) CuK-clinoptilolite. The lower part shows second-derivative spectra illustrating nitrogen hyperfine.

separated by 12.0 G can be seen clearly in the second-derivative spectrum.¹⁹ As shown in Figure 4, the nitrogen hyperfine lines in CuK–Clino are more clear than in CuNa–Clino, CuLi–Clino, or CuH–Clino.

Two main species are observed in CuH–Clino, CuLi–Clino, CuNa–Clino, and CuK–Clino for adsorbed pyridine (C₅D₅N). Nitrogen hyperfine lines are not observed in the g_{\perp} region. For CuH–Clino two Cu²⁺ species are clearly observed at $g_{||} =$

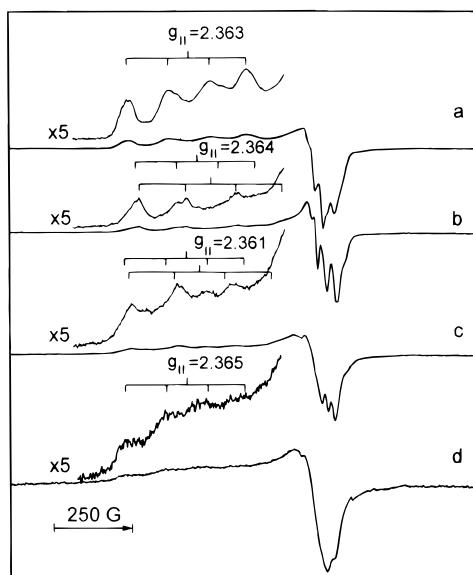


Figure 5. ESR spectra at 77 K after adsorption of acetonitrile (CD_3CN) on (a) CuH-clinoptilolite, (b) CuLi-clinoptilolite, (c) CuNa-clinoptilolite, and (d) CuK-clinoptilolite.

2.329, $A_{||} = 165 \times 10^{-4} \text{ cm}^{-1}$ and $g_{||} = 2.269$, $A_{||} = 184 \times 10^{-4} \text{ cm}^{-1}$ with the former dominant. CuLi-Clino shows similar results to CuH-Clino. The $g_{||}$ values of the two Cu^{2+} species in CuLi-Clino shift from 2.329 to 2.309 and from 2.269 to 2.317 compared to those observed in CuH-Clino. Two Cu^{2+} species in CuNa-Clino and CuK-Clino after $\text{C}_5\text{D}_5\text{N}$ adsorption are observed, similar to those in CuH-Clino. But the two species seem about equally abundant.

When acetonitrile is adsorbed onto CuH-Clino, one new Cu^{2+} species is formed with $g_{||} = 2.363$, $A_{||} = 146 \times 10^{-4} \text{ cm}^{-1}$ as shown in Figure 5. In contrast, the adsorption of CD_3CN onto CuLi-Clino results in the formation of two distinct Cu^{2+} species with $g_{||} = 2.364$ and $g_{||} = 2.304$. The $g_{||} = 2.364$ species is similar to the species in CuH-Clino. Two somewhat similar main species are also observed in CuNa-Clino with the $g_{||} = 2.361$ species dominant. In contrast, CuK-Clino shows a weak ESR intensity and only one Cu^{2+} species.

Ethylene (C_2D_4) adsorbed onto CuH-Clino, CuLi-Clino, CuNa-Clino, and CuK-Clino shows two Cu^{2+} -adsorbate species with similar intensities in CuH-Clino and CuLi-Clino. In CuNa-Clino and CuK-Clino the $g_{||} = 2.322$ and 2.314 species is dominant.

ESEM Studies. To get more information regarding the nature and location of the Cu^{2+} species during calcination, two-pulse ESEM experiments were performed at an external magnetic field corresponding approximately to the g_{\perp} position of the Cu^{2+} ESR spectrum, where the echo intensity reaches a maximum. In all samples there is a considerable reduction in the proton modulation depth with increasing calcination temperature. The modulation observed is mostly due to protons and aluminums.

The two-pulse Fourier transform (FT) ESEM spectra of CuH-Clino with different calcination temperatures are depicted in Figure 6A. The spectra consist of four peaks, one at 3.53–3.76 MHz corresponding to the aluminum Larmor frequency ν_{Al} , one sum harmonic peak in the region of $2\nu_{\text{Al}}$ (6.82–7.53 MHz), a peak at 13.7–14.1 MHz corresponding to the proton Larmor frequency ν_{H} , and another sum harmonic peak in the region of $2\nu_{\text{H}}$ (28.0–28.2 MHz). The more intense peak at $2\nu_{\text{H}}$ is due to protons with a very weak dipolar coupling that are not coordinated to Cu^{2+} .²⁵ As shown in Figure 6A, a fresh CuH-Clino sample shows relatively strong ν_{Al} and $2\nu_{\text{H}}$ peaks.

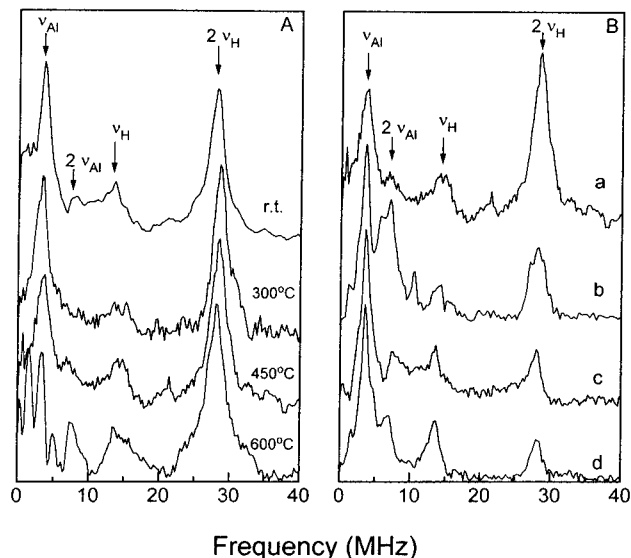


Figure 6. Fourier-transformed two-pulse ESEM spectra at 5 K and 3350 G for (A) CuH-clinoptilolite as a function of calcination temperature and (B) (a) CuH-clinoptilolite, (b) CuLi-clinoptilolite, (c) CuNa-clinoptilolite, and (d) CuK-clinoptilolite after calcination at 450 °C in air overnight.

After calcination at 300–600 °C in air, the $2\nu_{\text{H}}$ peak is still relatively strong, suggesting that calcined CuH-Clino rehydrated upon cooling in air.

In contrast, for CuLi-Clino, CuNa-Clino, or CuK-Clino the $2\nu_{\text{H}}$ peak intensity decreases, and the ν_{Al} peak intensity increases after calcination at 450 °C (Figure 6B). After calcination at 600 °C, the ν_{H} and $2\nu_{\text{H}}$ peaks are even smaller.

Figure 7 shows three-pulse deuterium ESEM spectra of CuH-Clino and CuK-Clino with adsorbed D_2O . The fit to CuK-Clino is reasonably good and clearly indicates coordination to two waters. For CuH-Clino the deuterium modulation is substantially deeper consistent with a larger water coordination number. The fit to $N = 6$ for CuH-Clino is not as good as the fit for CuK-Clino. Nevertheless, it seems convincing that the water coordination number is larger for CuH-Clino versus CuK-Clino, which is our major conclusion. The fits can be improved somewhat if N is not constrained to be integral, but we feel that this constraint is physically valid for first solvation shells. Overall, the ESEM spectral differences provide a convincing case for different water coordination numbers for CuH-Clino versus CuK-Clino. Table 3 shows similar differences for CuLi-Clino versus CuNa-Clino.

Three-pulse deuterium ESEM spectra from CuH-Clino and CuK-Clino after $\text{C}_2\text{H}_5\text{OD}$ adsorption are shown in Figure 8. CuH-Clino (Figure 8a) suggests three coordinated ethanols, even though the fit is only fair, while CuK-Clino shows only one. Again, the substantial difference in deuterium modulation depth clearly indicates different coordination numbers due to the different cocations. The simulation results in Table 3 for CuNa-Clino with adsorbed $\text{C}_2\text{H}_5\text{OD}$ show two coordinated ethanol molecules while for CuLi-Clino the ESEM spectra cannot be fitted well.

For adsorbed methanol (CD_3OH) Table 3 shows two coordinated methanols for CuNa-Clino but only one for CuK-Clino. Thus, there are substantial cocation effects on the adsorbate geometries.

Three-pulse ESEM spectra were recorded from CuH-Clino, CuLi-Clino, CuNa-Clino, and CuK-Clino with adsorbed ND_3 . The best fit to the experimental spectrum of CuH-Clino is $N = 12$ at $R = 0.27 \text{ nm}$ with $A_{\text{iso}} = 0.20 \text{ MHz}$, indicating that Cu^{2+} coordinates to four ammonia molecules. Although

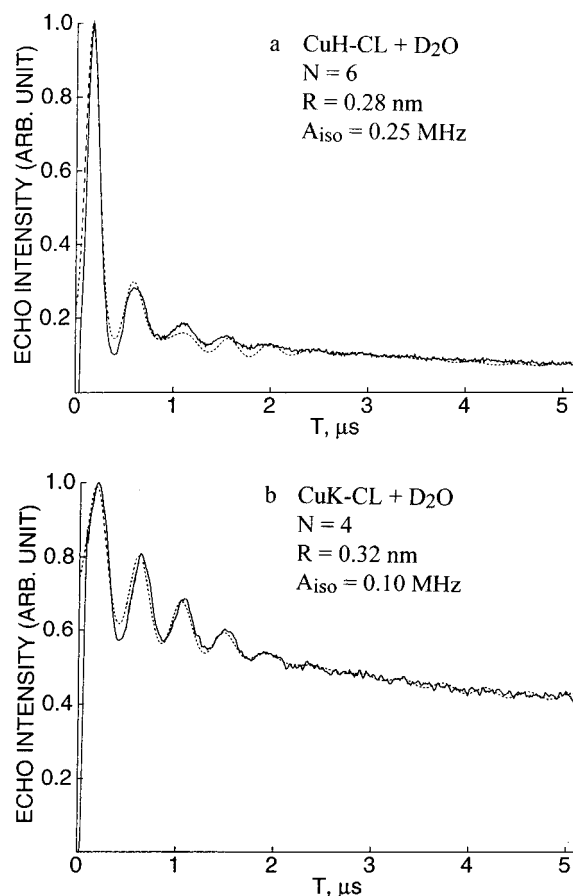


Figure 7. Experimental (—) and simulated (---) three-pulse ESEM spectra at 5 K of (a) CuH–clinoptilolite and (b) CuK–clinoptilolite with adsorbed water (D₂O).

TABLE 3: Number of Nuclei (N) and Interaction Distances (R , nm) Obtained from Simulation of ESEM Spectra at 5 K of Cupric Ion in Synthetic Clinoptilolite (A_{iso} in MHz)

adsorbate	parameter	cocation			
		H ⁺	Li ⁺	Na ⁺	K ⁺
D ₂ O	N	6	6	4	4
	R	0.28	0.30	0.30	0.32
	A_{iso}	0.25	0.27	0.25	0.10
CD ₃ OH	N			6	3
	R			0.36	0.34
	A_{iso}			0.17	0.14
C ₂ H ₅ OD	N	3		2	1
	R	0.30		0.29	0.30
	A_{iso}	0.36		0.37	0.33
ND ₃	N	12	12	9	9
	R	0.27	0.32	0.32	0.34
	A_{iso}	0.20	0.18	0.19	0.20
C ₅ D ₅ N	N_1	2			
	R_1	0.42			
	A_{iso}	0.19			
	N_2	3			
	R_2	0.51			
CD ₃ CN	N	~12	~12	~12	~12
	R	0.54	0.55	0.53	0.53
	A_{iso}	0.08	0.08	0.08	0.10
CD ₂ CD ₂	N	4			
	R	0.54			
	A_{iso}	0.10			

N can only be determined to ± 1 for $N \sim 12$, the overall fit seems more clearly consistent with four coordinated ammonias rather than a smaller number. Similar results are obtained for CuLi–Clino with a little longer Cu²⁺–D distance of 0.32 nm. But the CuNa–Clino/ND₃ and CuK–Clino/ND₃ spectra could

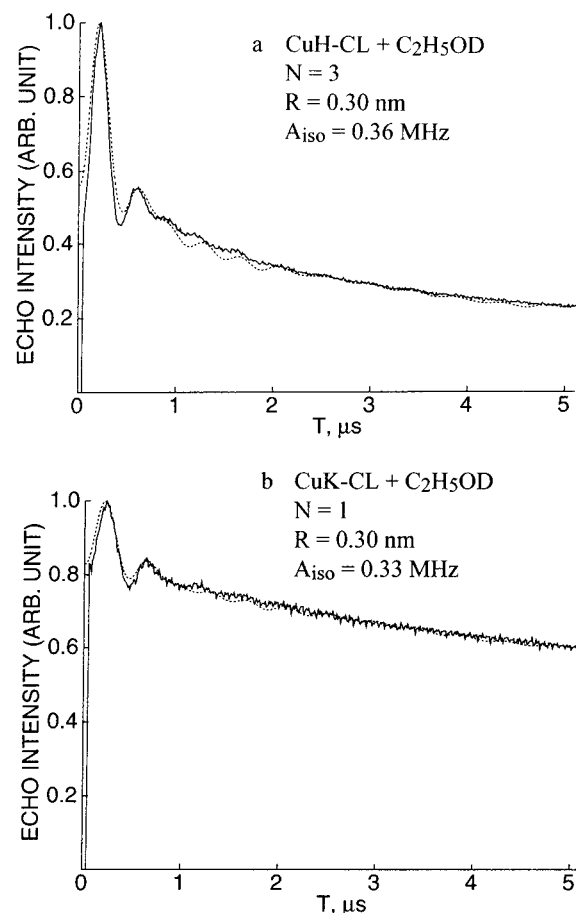


Figure 8. Experimental (—) and simulated (---) three-pulse ESEM spectra at 5 K of (a) CuH–clinoptilolite and (b) CuK–clinoptilolite with adsorbed ethanol (C₂H₅OD).

only be simulated with nine deuterium nuclei (three ammonia molecules) at $R = 0.32$ nm with $A_{iso} = 0.19$ MHz and $R = 0.34$ nm with $A_{iso} = 0.20$ MHz, respectively.

Figure 9 shows the three-pulse ESEM spectra of CuH–Clino and CuK–Clino with adsorbed CD₃CN. The spectra in Figure 9 do not contain strong modulation at short T which is characteristic of short-range interaction, but the modulation persists to long T which is indicative of longer range interaction. The spectrum is fit well by using $N = \sim 12$, at $R = 0.55$ nm with $A_{iso} = 0.08$ MHz. Similar results are obtained for CuLi–Clino, CuNa–Clino, and CuK–Clino as shown in Table 3. For $N = 12$ at this relatively long distance, similar fits are obtained for $N = 11$. However, the main point is that no change in acetonitrile coordination number with cocation is observed.

The three-pulse ESEM spectra for adsorption of C₅D₅N and CD₂CD₂ on CuH–Clino are shown in Figure 10. The simulation for C₅D₅N indicates interaction with two deuteriums in a first shell at $R = 0.42$ nm and three deuteriums in a second shell at a longer distance of 0.51 nm; thus, one molecule of pyridine coordinates to Cu²⁺. The simulation for CD₂CD₂ indicates interaction with four deuteriums; thus, one molecule of ethylene is coordinated with a Cu²⁺–D distance of 0.54 nm.

When C₅D₅N and CD₂CD₂ are adsorbed onto CuLi–Clino, CuNa–Clino, and CuK–Clino, only very weak deuterium modulation is detected and simulations were not reliable. The modulation depth increases in the following order: CuH–Clino \gg CuLi–Clino $>$ CuNa–Clino $>$ CuK–Clino for adsorption of both C₅D₅N and CD₂CD₂. This may reflect that the Cu²⁺–D distance decreases in the order CuH–Clino \ll CuLi–Clino $<$ CuNa–Clino $<$ CuK–Clino.

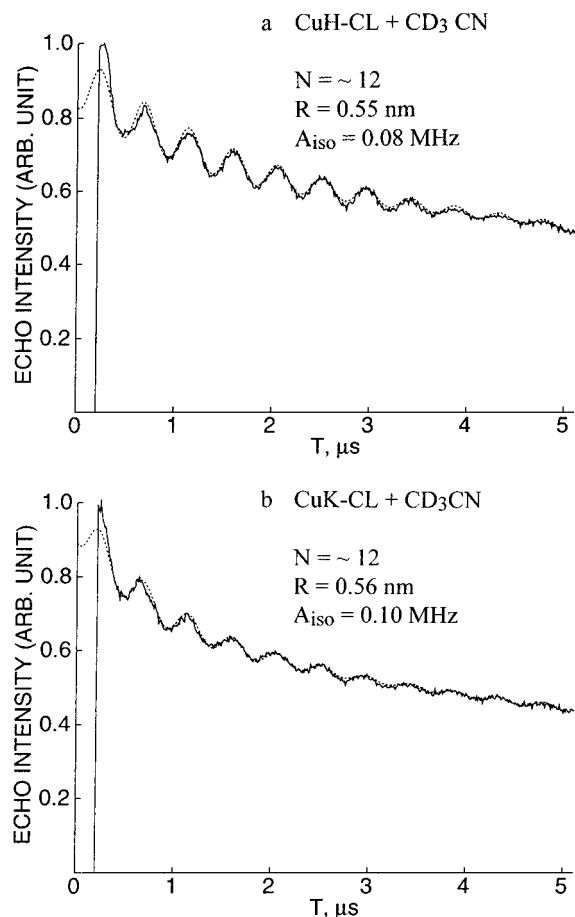


Figure 9. Experimental (—) and simulated (---) three-pulse ESEM spectra at 5 K of (a) CuH-clinoptilolite and (b) CuK-clinoptilolite with adsorbed acetonitrile (CD_3CN).

Discussion

Several crystallographic studies have been done to determine the locations of various cations in both hydrated and dehydrated clinoptilolite.^{26–29} Clinoptilolite has two main channels termed A (ten-member ring) and B (eight-member ring) parallel to each other and to the c -axis of the unit cell, while C channels (eight-member ring) lie along the a -axis intersecting the A and B channels.¹⁴ Possible cation sites are M1, M2, M3, and M4²² as illustrated in Figure 11. In the M1 and M2 sites, the cation is coordinated by framework oxygens plus some water molecules and is offset in channels A and B. In the M3 site, the cation is located in intersecting channel C coordinated with framework oxygens plus some water. In the M4 site the cation is located at the center of channel A and is fully coordinated with water molecules.²²

In fresh CuH-Clino two anisotropic Cu^{2+} species are observed at 77 K (Figure 1a). The ESR recorded at room temperature exhibits a broader signal with copper hyperfine indicative of an immobile species.²⁰ The two-pulse FT-ESEM (Figure 6A) shows a strong ν_{Al} peak, even in room temperature, indicating that the Cu^{2+} is directly associated with zeolitic aluminum.^{20,25} ESR shows that CuH-Clino after calcination at 300–600 °C in air and rehydration loses one of the Cu^{2+} species. ESEM results for CuH-Clino indicate that cupric ion is coordinated to three water molecules. After evacuation at room temperature, the ESR spectra show that the relative intensities of the two Cu^{2+} species change, but the same ESEM result is obtained. This suggests that two cupric species designated Cu_{III} are coordinated to three water molecules in sites with different geometries which could be the M1 and M2 sites.

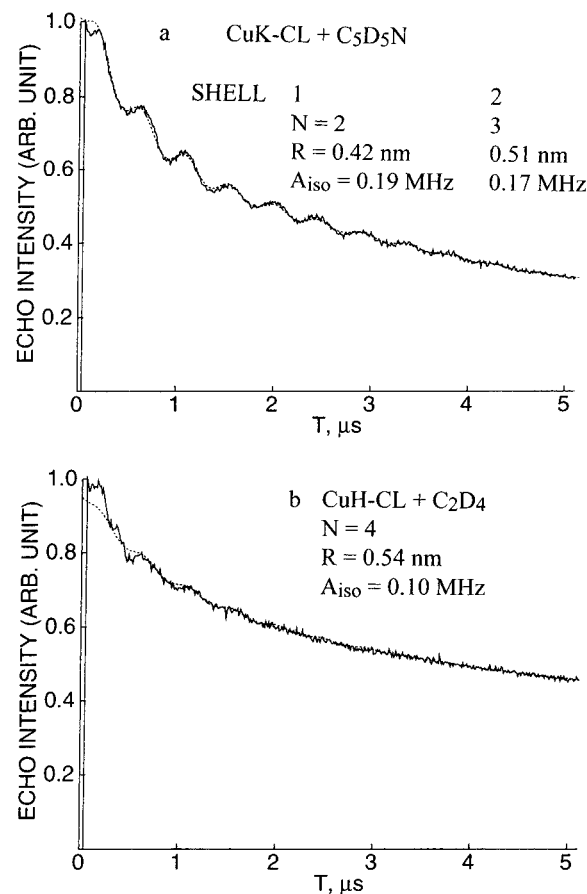


Figure 10. Experimental (—) and simulated (---) three-pulse ESEM spectra recorded at 5 K of CuH-clinoptilolite with adsorbed (a) pyridine ($\text{C}_5\text{D}_5\text{N}$) and (b) ethylene (CD_2CD_2).

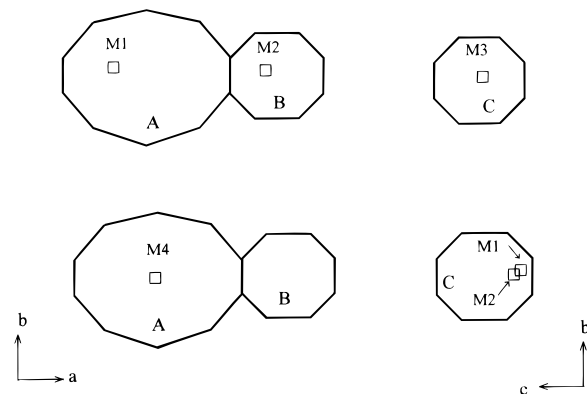


Figure 11. Cation locations M1 to M4 shown schematically in the clinoptilolite channels. The intersections represent Si or Al with framework oxygens in between and the squares represent cation sites. Adapted from ref 22.

The ESR results suggest that part of the cupric ions can migrate from one site to another.

As fresh CuH-Clino is dehydrated to 400 °C the g_{\parallel} and A_{\parallel} values change to those characteristic of Cu_0 , corresponding to loss of water ligands and coordination only to the zeolite lattice.^{30,31} It is also noted that the transition from Cu_{III} to Cu_0 appears to proceed via an intermediate species, probably corresponding to partial loss of water molecules. The most probable position for Cu_0 is in smaller channel C in a M3 site to enable coordination to oxygens on both sides.

Fresh CuNa-Clino and CuK-Clino also show two cupric species. ESR spectra at room temperature exhibit copper hyperfine indicating immobile Cu^{2+} , although another apparently isotropic species at $g_1 = 2.163$ is also present. ESEM

results indicate that cupric ion is coordinated to two molecules of water in fresh CuNa—Clino and after rehydration. Cu^{2+} in CuNa—Clino and CuK—Clino is also suggested to be located at M1 and M2 sites. After calcination at 450 or 600 °C in air only one main Cu^{2+} species remains (Figure 1B). When fresh CuNa—Clino and CuK—Clino are dehydrated, their ESR parameters change consistent with Cu_{III} losing its water molecules.^{30,31}

From the ESEM and ESR results, ion—adsorbate cupric complexes in H—CL and Li—CL differ from those Na—CL and K—CL. For fresh CuH—Clino and CuLi—Clino, cupric ion is coordinated to three water molecules, but only to two waters in CuNa—Clino and CuK—Clino. The larger cocations appear to decrease the water coordination number for cupric ion.

The adsorption of both polar and nonpolar molecules shows further differences between Cu^{2+} in CuH—Clino versus CuNa—Clino and CuK—Clino. From ESEM results, cupric ion coordinates four molecules of ammonia in CuH—Clino and CuLi—Clino, but only three ammonia molecules in CuNa—Clino and CuK—Clino. The nitrogen hyperfine splitting indicates that Cu^{2+} directly interacts with the nitrogen of an ammonia ligand. This has been observed previously with Cu^{2+} — NH_3 complexes in zeolites.²¹ So small cocations can provide enough free space to accommodate Cu^{2+} —ammonia complexes with four or three ammonia molecules, probably at M1 sites.

The adsorption of ethanol onto CuH—Clino results in two cupric species, but with CuNa—Clino and CuK—Clino only one species is observed. ESEM results indicate that the cupric ion coordinates three molecules of ethanol in CuH—Clino, but only two or one ethanols in CuNa—Clino and CuK—Clino, respectively. The Cu^{2+} —O bond length calculated from the ESEM results is 0.23 nm, which agrees with the Cu^{2+} —(O) H_2O distance of 0.233 nm.³² Thus, cupric ion is directly coordinated to ethanol through the hydroxyl oxygen. The ethanol coordination number of three in CuH—Clino is the same as for water as a ligand.

The Cu^{2+} —ethanol complexes formed in CuNa—Clino and CuK—Clino are virtually identical with each other with respect to ESEM and ESR parameters. Similar results with adsorbed methanol support that cupric ion is coordinated to two and one molecules of methanol in CuNa—Clino and CuK—Clino, respectively. The cocation size seems more important than adsorbate size for controlling the adsorbate complex formed.

With adsorbed acetonitrile, one Cu^{2+} species is detected by ESR in CuH—Clino and CuK—Clino while two Cu^{2+} species are observed in CuLi—Clino and CuNa—Clino. However, the ESEM spectra show the same number of coordinated molecules for all cocations. The Cu^{2+} —D distance is about 0.53–0.55 nm, but this corresponds to a Cu^{2+} —N(CD_3CN) distance of about 0.23–0.25 nm, indicating that cupric ion is directly coordinated with four acetonitrile molecules. Since the cocation does not affect the number of coordinated acetonitrile molecules, a large site is implied which suggests an M4 site (see Figure 12). This suggests that the migration of a cupric ion from M2 or M3 sites to an M4 site occurs with a strong coordinating ligand.

Adsorption of pyridine onto CuH—Clino forms two Cu^{2+} species. The species with $A_{\text{H}} = 165 \times 10^{-4} \text{ cm}^{-1}$ is assigned to Cu_0 , and the other is assigned to a pyridine complex. ESEM results show cupric ion coordination to one molecule of pyridine with separate average distances to two sets of deuteriums in this molecule. The shortest distance of 0.42 nm (Table 3) indicates a weak interaction which seems consistent with no ESR observation of nitrogen hyperfine. Adsorption of pyridine onto CuNa—Clino, CuLi—Clino, and CuK—Clino gives deu-

terium modulation too weak to analyze so we surmise that the interaction with pyridine must be even weaker than for CuH—Clino.

Ethylene is the only nonpolar adsorbate investigated. ESR results (Table 2) show that two Cu^{2+} species are formed in all samples. The Cu^{2+} species with $A_{\text{H}} \sim 168 \times 10^{-4} \text{ cm}^{-1}$ is similar to the Cu^{2+} species after complete dehydration and is assigned to Cu_0 uncoordinated to any waters. The observation of a Cu_0 species indicates that not all of the cupric ion sites are accessible to ethylene. ESEM results for CuLi—Clino, CuNa—Clino, and CuK—Clino show deuterium modulation too weak to be simulated, indicating that cupric ion is not directly coordinated to ethylene. For CuH—Clino, ESEM results show one ethylene coordinated with a Cu^{2+} —D distance of 0.54 nm. On the basis of other Cu^{2+} —ethylene complexes in zeolites, this is consistent with π -bonding coordination to ethylene.

Conclusions

At low Cu^{2+} loading in hydrated synthetic clinoptilolite, Cu^{2+} is coordinated to three water molecules in CuH—clinoptilolite (CuH—Clino) and in CuLi—Clino but only to two water molecules in CuNa—Clino and CuK—Clino. These species locate in the main channels in M1 and M2 sites and also coordinate to oxygens of the zeolite lattice. Evacuation is sufficient to cause water loss from the complex. Complete dehydration is effected at 250–400 °C, and then the Cu^{2+} migrates to intersecting channel site M3.

Adsorption of polar molecules such as water, alcohols, ammonia, and acetonitrile causes the Cu^{2+} to migrate back into the main channel and form adsorbate complexes. Less polar molecules such as ethylene and pyridine are slower at effecting migration of the Cu^{2+} . The adsorbate coordination number of the Cu^{2+} complexes is greatly affected by the cocation in clinoptilolite. Cupric ion coordinates to three molecules of ethanol, four of ammonia, and one of pyridine in CuH—Clino but to only two molecules of methanol or ethanol and three of ammonia in CuNa—Clino and one molecule of methanol or ethanol and three of ammonia in CuK—Clino. Four molecules of acetonitrile coordinate to cupric ion in all samples. No cocation effect is noted for acetonitrile complexes, and the most probable site for these complexes is in the M4 site in the center of a main channel.

Acknowledgment. This research was supported by the National Science Foundation and the Robert A. Welch Foundation.

References and Notes

- (1) Tsuruya, S.; Tsukamoto, M.; Watanabe, M.; Masai, M. *J. Catal.* **1985**, *93*, 303.
- (2) Benn, F. R.; Dwyer, J.; Estahami, A.; Evmerides, N. P.; Szczepura, A. K. *J. Catal.* **1977**, *48*, 60.
- (3) Naccache, C. M.; Taarit, Y. B. *J. Catal.* **1971**, *22*, 171.
- (4) Maxwell, I. E.; Downing, R. S.; van Langen, S. A. *J. Catal.* **1980**, *61*, 485.
- (5) Tsutsumi, K.; Fuji, S.; Takahashi, H. *J. Catal.* **1977**, *24*, 146.
- (6) (a) Iwamoto, M.; Yahiro, H.; Mizuno, N.; Zhang, W.-X.; Mine, Y.; Furukawa, H.; Kagawa, S. *J. Phys. Chem.* **1992**, *96*, 9360. (b) Shelef, M. *Chem. Rev.* **1995**, *95*, 209.
- (7) Ichikawa, T.; Kevan, L. *J. Am. Chem. Soc.* **1983**, *105*, 402.
- (8) Narayana, M.; Kevan, L. *J. Chem. Phys.* **1983**, *87*, 3573.
- (9) Ichikawa, T.; Kevan, L. *J. Phys. Chem.* **1983**, *78*, 4433.
- (10) Herman, R. G.; Flentge, D. R. *J. Phys. Chem.* **1978**, *82*, 720.
- (11) Herman, R. G. *Inorg. Chem.* **1979**, *18*, 995.
- (12) Kevan, L. In *Time Domain Electron Spin Resonance*; Kevan, L., Schwartz, R. N., Eds.; Wiley-Interscience: New York, 1979; Chapter 8.
- (13) Fauth, J. M.; Schweiger, A.; Brauschweiler, L.; Forrer, J.; Ernst, R. R. *J. Magn. Reson.* **1986**, *66*, 74.
- (14) Gottardi, G.; Galli, E. *Natural Zeolites*; Springer-Verlag: Berlin, 1985; p 256.

- (15) Vaughan, D. E. W. In *Natural Zeolites: Occurrence, Properties, Use*; Sand, L. B., Mumpton, F. A., Eds.; Pergamon: Oxford, 1978; pp 353–371.
- (16) Leppert, D. *Min. Eng. (Littleton, Colo.)* **1990**, 42, 604.
- (17) Woo, H. C.; Lee, K. H.; Lee, J. S. *Appl. Catal. A* **1996**, 134, 147.
- (18) Zhao, D.; Szostak, R.; Kevan, L. Submitted for publication.
- (19) Sass, C. E.; Kevan, L. *J. Phys. Chem.* **1988**, 92, 5192.
- (20) Anderson, M. E.; Kevan, L. *J. Phys. Chem.* **1987**, 91, 4174.
- (21) Sass, C. E.; Kevan, L. *J. Phys. Chem.* **1989**, 93, 4669.
- (22) Ackley, M. W.; Giese, R. F.; Yang, R. T. *Zeolites* **1992**, 12, 780.
- (23) Kevan, L.; Bowman, M. K.; Narayana, P. A.; Boeckman, R. K.; Yudanov, V. F.; Tsvetkov, Yu. D. *J. Chem. Phys.* **1975**, 63, 409.
- (24) Mumpton, F. A. *Am. Mineral.* **1972**, 57, 1463.
- (25) Matar, K.; Zhao, D.; Goldfarb, D.; Azelee, W.; Daniel, W.; Harrison, P. G. *J. Phys. Chem.* **1995**, 99, 9966.
- (26) Bresciani-Pahor, N.; Calligaris, M.; Nardin, G.; Randaccio, L.; Russo, E.; Comin-Chiaramonti, P. *J. Chem. Soc., Dalton Trans.* **1980**, 1511.
- (27) Bresciani-Pahor, N.; Calligaris, M.; Nardin, G.; Randaccio, L. *J. Chem. Soc., Dalton Trans.* **1981**, 2288.
- (28) Galli, E.; Gottardi, G.; Mayer, H.; Preisinger, A.; Passaglia, E. *Acta Crystallogr.* **1983**, B39, 189.
- (29) Koyama, K.; Takeuchi, Y. *Z. Kristallogr.* **1977**, 145, 216.
- (30) Anderson, M. W.; Kevan, L. *J. Phys. Chem.* **1986**, 90, 3206.
- (31) Anderson, M. W.; Kevan, L. *J. Phys. Chem.* **1987**, 91, 2926.
- (32) Elson, J.; King, G. S. D.; Mortier, W. J. *J. Phys. Chem.* **1987**, 91, 5800.